World Journal of Engineering and Technology, 2026, 14(2), 344-356
https://www.scirp.org/journal/wjet
ISSN Online: 2331-4249
ISSN Print: 2331-4222

Analysis of Error Results from Three-Dimensional Coordinate Measuring Machine for Detecting Precision Machined Components of Rotating Bodies

Ning Wu, Na Li, Teng Zhang, Yahui Wen

Xi'an Refra Tungsten & Molybdenum Co., Ltd., Xi'an, China
Email: ningwu84@126.com

How to cite this paper: Wu, N., Li, N., Zhang, T. and Wen, Y.H. (2026) Analysis of Error Results from Three-Dimensional Coordinate Measuring Machine for Detecting Precision Machined Components of Rotating Bodies. *World Journal of Engineering and Technology*, **14**, 344-356.
https://doi.org/10.4236/wjet.2026.142020

Received: January 26, 2026
Accepted: March 28, 2026
Published: March 31, 2026

Abstract

With the development of high-tech, the construction of intelligent production lines, and the advancement of the Industry 4.0 era, the demand for high-end products is increasing. As China's requirements for part machining accuracy are continuously upgraded and the scale of mass production expands, the demands for the accuracy and efficiency of part measurements are becoming higher. As a high-precision inspection equipment, the coordinate measuring machine (CMM) fully meets the requirements of modern industry in terms of inspection accuracy and efficiency. Therefore, using CMMs for part inspection is imperative. Currently, CMM inspection is one of the main methods for detecting dimensional tolerances, form tolerances, location tolerances, and orientation tolerances of parts. Its advantages are high accuracy, good repeatability, high efficiency, and low cost. This paper analyzes the measurement results of flatness of planes themselves, parallelism between planes, perpendicularity between cylinders and planes, and position tolerance between cylinders and planes and between cylinders in rotary parts. It summarizes the main causes of errors and provides suggestions and recommendations for subsequent inspection directions.

Keywords

Three-Coordinate Measuring Machine, Error, Flatness, Perpendicularity, Parallelism, Position Accuracy, Rotating Body

1. Introduction

China's manufacturing industry is rapidly developing towards scale, digitalization, and high precision. To achieve the upgrade from "rough machining" to "precision manufacturing," promote mass production, and improve the inspection efficiency of mass production, CMMs, as digital, traceable high-precision inspection equipment, are widely used in various industries [1]-[3]. Currently, CMMs are mainly used to inspect small precision machined parts, conventional mechanical parts such as shafts, large structural parts, surface/complex contour parts, automotive parts, and easily deformable parts [4] [5]. Although the inspection accuracy of CMMs has reached as high as ±1 μm, and their accuracy in inspecting complex geometric tolerances such as flatness, position tolerance, and parallelism is far superior to traditional measuring tools, the measurement values of CMMs are still subject to deviations due to various influencing factors [6]. This paper analyzes the measurement results of dimensional accuracy of cylinders, flatness of planes, parallelism between surfaces, perpendicularity between cylinders and surfaces, and position tolerance of cylinders in rotary parts. It summarizes the main causes of errors and provides suggestions and recommendations for subsequent inspection directions.

2. Introduction to Tolerances

In the mechanical industry, tolerance refers to the maximum allowable variation of actual geometric parameters. The purpose of designers specifying tolerances is to ensure the interchangeability of parts and to ensure the assembly performance and service performance of mechanical products [7] [8]. Tolerances include dimensional tolerances, form tolerances, position tolerances, orientation tolerances, etc. Among them, dimensional tolerances are used to control the actual size of the measured feature, controlling the deviation between the actual size and the theoretical size, such as the distance between surfaces, the diameter of holes, etc.; form tolerances are used to control the form error of the measured feature itself, controlling the deviation of the measured feature from the theoretical shape, such as straightness, flatness, cylindricity, etc.; position tolerances are used to define the allowable variation of the actual position of the measured feature relative to the ideal position, such as the coaxiality between cylinders, the position accuracy of cylinders, etc.; orientation tolerances are used to define the allowable variation of the actual orientation of the measured element relative to the theoretical orientation, such as the parallelism between surfaces, the perpendicularity between cylinders and surfaces, etc. [9] [10]. Dimensional tolerances and form tolerances only consider the feature itself and do not need to constrain the relationship with the datum; position tolerances and orientation tolerances need to constrain the relationship with the datum, otherwise they cannot be evaluated [11].

3. Introduction to Basic Elements

Datums in CMM inspection include geometric features such as points, lines, and planes. Datums serve the following purposes: 1) Provide a reference for evaluating the location and orientation tolerances of measured features; 2) Ensure consistency between the inspection datum, design datum, and process datum, avoiding measurement errors caused by datum inconsistency; 3) Restrict the spatial degrees of freedom of the part through the combination of multiple datums, ensuring the measurement posture aligns with the design requirements.

4. Part Inspection and Data Analysis

This study relies on a Hexagon CMM, model Global Plus, with a measuring range of 600 mm × 1000 mm × 600 mm, a repeatability of 1.5 μm, an inspection temperature requirement of 20˚C ± 2˚C, and a calculation method using the least squares method (this method ensures measurement results are not affected by individual outliers, and the calculation results are unique and reproducible). During the inspection process, the temperature was consistently maintained between 20˚C and 22˚C, and the inspection environment was free from contamination, dust, vibration, and other influencing factors.

4.1. Inspection Data

4.1.1. Detection of Datum A Flatness

This round is divided into two situations for verification. The first situation verifies the relationship between Datum A flatness and the number of sampling points. The second situation verifies the relationship between Datum A flatness and sampling point positions when the number of sampling points remains unchanged. The positional relationship of Datum A is shown in **Figure 1**, and the part clamping method and probe direction are shown in **Figure 2**.

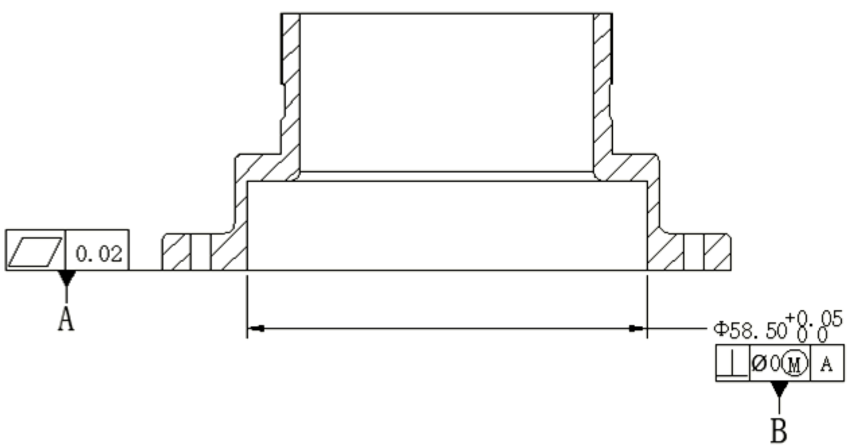

Figure 1. Schematic diagram of the positional relationship between Datum A and Datum B.

First situation: The number of sampling points and their positions are divided into three states. State 1: Datum A has 4 evenly distributed sampling points; State 2: Datum A has 8 evenly distributed sampling points; State 3: Datum A has 12 evenly distributed sampling points. The starting position of sampling points is in the (0, 0, −1) vector direction. Four sets of data were measured for each state. The measured values of Datum A flatness at this time are shown in Table 1.

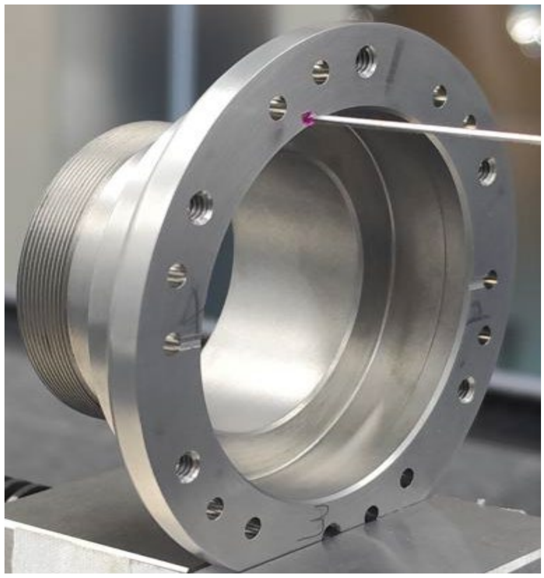

Figure 2. Schematic diagram of the part clamping method and probe angle during Datum A inspection.

Table 1. Measured values of Datum A flatness with different numbers of sampling points.

Comparison Dimension	A: 4 Points		A: 8 Points		A: 12 Points	
A Flatness (mm) ⏥ 0.02	0.0091	0.0091	0.0096	0.0096	0.0105	0.0105
	0.0091	0.0091	0.0097	0.0096	0.0105	0.0105
A Avg Flatness (mm)	0.0091		0.0096		0.0105	
Range of A Flatness (mm)	0		0.0001		0	

As can be seen from the data in Table 1, when the number of sampling points is the same, the maximum deviation of the Datum A flatness measurement value is only 0.0001 mm, which is far less than the equipment's repeatability; when the number of sampling points is evenly distributed 4, the mean Datum A flatness is the smallest at 0.0091 mm; when the number of sampling points is evenly distributed 8, the mean Datum A flatness is 0.0096 mm; when the number of sampling points is evenly distributed 12, the mean Datum A flatness is the largest at 0.0105 mm. The data shows that the Datum A flatness measurement value increases with the increase in the number of sampling points.

Second situation: Datum A has 6 evenly distributed sampling points. The starting positions of the sampling points are divided into two states. In state 1, the starting position of the sampling points is in the (0, 0, −1) vector direction; in state 2, the starting position of the sampling points is in the (1, 0, 0) vector direction. Four sets of data were measured for each state. The measured values of Datum A flatness at this time are shown in Table 2.

Table 2. Measured values of Datum A flatness with the same number of sampling points but different positions.

Comparison Dimension	A Evenly Distributed Sampling Points, 6 points			
	Starting Point in (0, 0, −1)		Starting Point in (1, 0, 0)	
A Flatness (mm) ⏥ 0.02	0.0099	0.0100	0.0074	0.0074
	0.0100	0.0088	0.0074	0.0074
A Avg Flatness (mm)	0.0097		0.0074	
Range of A Flatness (mm)	0.0012		0	

As can be seen from the data in Table 2, after changing the number and position of sampling points, the Datum A flatness measurement value changed, with an average difference of 0.0023 mm. This is because the sampling point position of Datum A changed. Therefore, when subsequent measurement values need to refer to Datum A, the number and position of Datum A sampling points will be fixed.

4.1.2. Detection of Datum B Diameter and Perpendicularity

The detection of Datum B diameter and perpendicularity is divided into two situations for verification. The first situation is to change the number and position of Datum A sampling points while keeping the number and position of Datum B sampling points unchanged. The second situation is to keep the number and position of Datum A sampling points unchanged while changing the number and position of Datum B sampling points.

First situation: Detect the perpendicularity of Datum B when the state of Datum A changes while the state of Datum B remains unchanged. The positional relationship between Datum A and Datum B is shown in Figure 1. During the detection process, the number of Datum B sampling points is 8 evenly distributed in a single layer, with a total of 2 layers. The starting position of the sampling points is in the (0, 0, −1) direction (at this time, the measured diameter of cylinder B is φ58.5232 mm, and the perpendicularity requirement is less than 0.0268 mm). The detection process is divided into three states, and four sets of data were measured for each state. State 1: Datum A has 4 evenly distributed sampling points; State 2: Datum A has 8 evenly distributed sampling points; State 3: Datum A has 12 evenly distributed sampling points. The measured values of Datum B perpendicularity are shown in Table 3.

From the data in Table 3 (Datum A flatness data comes from Table 1), it can be seen that when the number and position of Datum A sampling points remain unchanged, the maximum deviation of the perpendicularity measurement value is 0.0008 mm, which is less than the equipment's repeatability; when the number and position of Datum A sampling points change, the difference between the maximum and minimum mean values of perpendicularity is only 0.0004 mm. The data in the table shows that there is no correlation between the magnitude of Datum B perpendicularity and the magnitude of Datum A flatness.

Table 3. Measured values of Datum B perpendicularity when Datum A state changes and Datum B state remains unchanged.

Comparison Dimension	A: 4 Points		A: 8 Points		A: 12 Points	
	B Single Layer Distributed 8 points, 2 Layers, Starting Point in (0, 0, −1)					
A Avg Flatness (mm) ▱ 0.02	0.0091		0.0096		0.0105	
Range of A Flatness (mm)	0		0.0001		0	
B Perpendicularity (mm) ⊥ Ø0 Ⓜ A	0.0045	0.0037	0.0040	0.0036	0.0036	0.0041
	0.0042	0.0041	0.0040	0.0039	0.0036	0.0039
B Avg Perpendicularity (mm)	0.0041		0.0038		0.0038	
Range of B Perpendicularity (mm)	0.0008		0.0004		0.0005	

Second situation: Detect the diameter and perpendicularity of Datum B when the state of Datum A remains unchanged and the state of Datum B changes. During the detection process, the number of Datum A sampling points is 8 evenly distributed, and the starting position of the sampling points is in the (0, 0, −1) direction (at this time, the flatness of Datum A is 0.0096 mm). The layout of Datum B sampling points is divided into three states, and four sets of data were measured for each state. State 1: Datum B sampling points are 4 evenly distributed in a single layer, with a total of 2 layers; State 2: Datum B sampling points are 8 evenly distributed in a single layer, with a total of 2 layers; State 3: Datum B sampling points are 12 evenly distributed in a single layer, with a total of 2 layers. The measured values of Datum B diameter and perpendicularity are shown in Table 4.

Table 4. Measured values of Datum B diameter and perpendicularity when Datum A state remains unchanged and Datum B state changes.

Comparison Dimension	A Evenly Distributed 8 Points, Starting Point in (0, 0, −1)					
	B Single Layer 4 Points 2 Layers		B Single Layer 8 Points Layers		B Single Layer 12 Points Layers	
B Diameter ($\phi 58.5^{+0.05}_{0}$ mm)	58.5234	58.5235	58.5232	58.5231	58.5233	58.5232
	58.5233	58.5233	58.5233	58.5232	58.5231	58.5233
B Avg Diameter (mm)	58.5234		58.5232		58.5232	
Range of B Diameter (mm)	0.0002		0.0002		0.0002	
B Perpendicularity (mm) ⊥ Ø0 Ⓜ A	0.0044	0.0046	0.0040	0.0036	0.0049	0.0050
	0.0045	0.0048	0.0040	0.0039	0.0048	0.0047
B Avg Perpendicularity (mm)	0.0046		0.0038		0.0049	
Range of B Perpendicularity (mm)	0.0004		0.0004		0.0003	

From the data in Table 4, it can be seen that when the number and position of Datum B sampling points remain unchanged, the maximum range of Datum B diameter is 0.0002 mm, and the maximum range of Datum B perpendicularity is

0.0004 mm, both far less than the equipment's repeatability; when the number and position of Datum B sampling points change, the difference between the maximum and minimum mean values of Datum B diameter is 0.0002 mm, and the difference between the maximum and minimum mean values of Datum B perpendicularity is 0.0011 mm. The data results show that when the number of Datum B sampling points is 8 per layer × 2 layers, the perpendicularity is the smallest, and the perpendicularity is similar in the other two cases.

4.1.3. Detection of Datum C Flatness, Parallelism, and Datum D Position Tolerance

This round detects the flatness and parallelism of Datum C and the position accuracy of Datum D under the condition that both Datum A and Datum B states remain unchanged. As can be seen from **Figure 2**, Datum C and Datum D can only sample within half a circular surface and half a cylindrical surface. The positional relationship between Datum C, Datum D, Datum A, and Datum B is shown in **Figure 3**. The probe direction during the detection of Datum C and Datum D is shown in **Figure 4**.

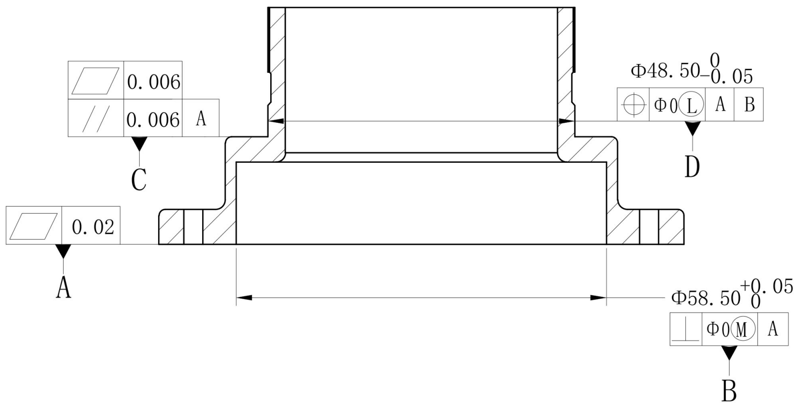

Figure 3. Schematic diagram of the positional relationship among Datum C, Datum D, Datum A, and Datum B.

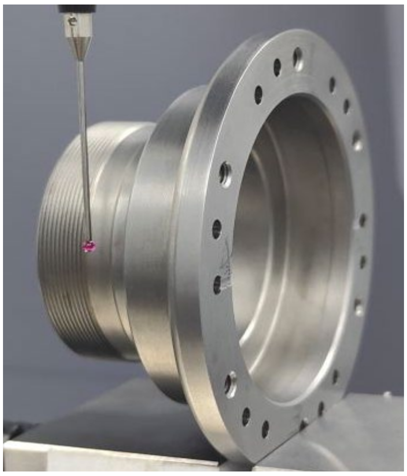

Figure 4. Schematic diagram of the probe angle during inspection of Datum C and D.

In this round of detection, Datum A has 8 evenly distributed sampling points, and Datum B has 8 evenly distributed sampling points per layer, with a total of 2 layers (the flatness of Datum A is 0.0096 mm, and the perpendicularity of Datum B is 0.0038 mm). This round of detection is divided into three states. In state 1, Datum C has 5 sampling points, and Datum D has 4 evenly distributed sampling points per layer, with a total of 2 layers; in state 2, Datum C has 8 sampling points, and Datum D has 6 evenly distributed sampling points per layer, with a total of 2 layers; in state 3, Datum C has 11 sampling points, and Datum D has 8 evenly distributed sampling points per layer, with a total of 2 layers. The measured values of Datum C flatness, parallelism, and Datum D position accuracy are shown in Table 5.

Table 5. Measured values of Datum C flatness, parallelism, and Datum D position accuracy.

Comparison Dimension	A Evenly Distributed 8 Points, Starting Point in (0, 0, −1)					
	B Single Layer 8 Points, 2 Layers, Starting Point in (0, 0, −1)					
	C: 5 Points		C: 8 Points		C: 11 Points	
	D Single Layer 4 Points 2 Layers		D Single Layer 6 Points 2 Layers		D Single Layer 8 Points 2 Layers	
C Flatness (mm) ⏥ 0.006	0.0042	0.0041	0.0045	0.0045	0.0055	0.0055
	0.0042	0.0042	0.0045	0.0045	0.0055	0.0055
C Avg Flatness (mm)	0.0042		0.0045		0.0055	
Range of C Flatness (mm)	0.0001		0		0	
C Parallelism (mm) // 0.006 A	0.0117	0.0116	0.0118	0.0118	0.0130	0.0130
	0.0116	0.0117	0.0118	0.0117	0.0130	0.0129
C Avg Parallelism (mm)	0.0117		0.0118		0.0130	
Range of C Parallelism (mm)	0.0001		0.0001		0.0001	
D Diameter ($48.5^{0}_{-0.05} mm$)	48.4832	48.4830	48.4837	48.4837	48.4841	48.4840
	48.4830	48.4831	48.4837	48.4836	48.4840	48.4840
D Avg Diameter (mm)	48.4831		48.4837		48.4840	
Range of D Diameter (mm)	0.0002		0.0001		0.0001	
D Position Accuracy (mm) ⌖ Ø0 Ⓛ A B	0.0255	0.0260	0.0267	0.0267	0.0293	0.0298
	0.0264	0.0263	0.0266	0.0262	0.0291	0.0301
D Avg Position Accuracy (mm)	0.0261		0.0266		0.0296	
Range of D Position Accuracy (mm)	0.0009		0.0005		0.0010	

The data in Table 5 shows that when the number and position of sampling points remain unchanged, the maximum range of Datum C flatness is 0.0001 mm, the maximum range of Datum C parallelism is 0.0001 mm, and the maximum range of Datum D position accuracy is 0.0010 mm, all of which are less than the equipment's repeatability. The measurement values are stable, consistent with the results of the previous three rounds of verification.

In the case where the number of Datum C sampling points increases from 5 to 11, the Datum C flatness increases from 0.0042 mm to 0.0055 mm, with an increment of 0.0013 mm; the Datum C parallelism increases from 0.0117 mm to 0.0130 mm, with an increment of 0.0013 mm; the Datum D position accuracy increases from 0.0261 mm to 0.0296 mm, with an increment of 0.0033 mm. Combined with the measurement values from the previous three rounds, it can be seen that the number and position of sampling points have a certain influence on the measurement values. The data shows that both Datum C flatness and Datum D position accuracy increase with the increase in the number of sampling points, and the variation pattern of Datum C flatness is consistent with that of Datum A flatness measurement values.

4.1.4. Influence of Clamping Angle on the Measurement Values of Datum A Flatness, Datum B Diameter, and Perpendicularity

This round verifies the influence of clamping angle on the measurement values of Datum A flatness, Datum B diameter, and perpendicularity. The workpiece clamping angles are divided into four directions, with specific positions shown in **Figure 5**. When detecting a certain angle, that angle is clamped at the position shown in **Figure 5**. Four sets of data were measured for each of the workpiece clamping angles at 0˚, 90˚, 180˚, and 270˚. In the previous rounds of detection, the clamping angle was always at the 0˚ position, so this round only measures data for the other three angles.

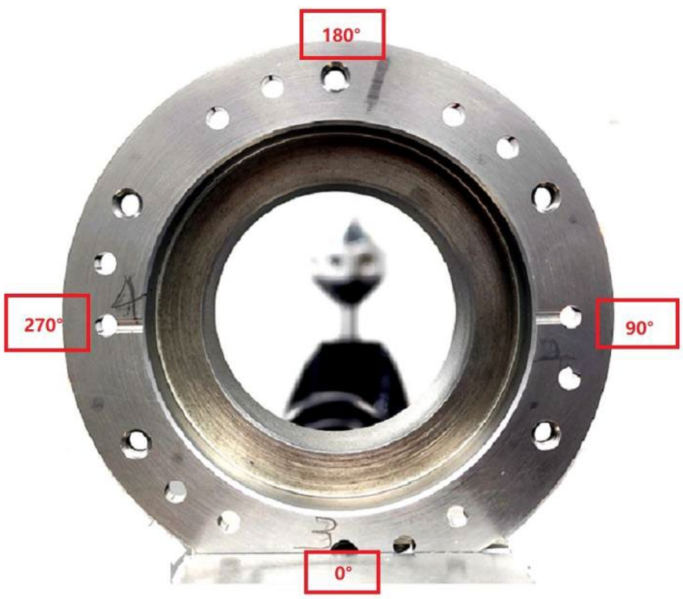

Figure 5. Schematic diagram of clamping angles.

During the detection process, Datum A has 8 evenly distributed sampling points, and Datum B has 8 evenly distributed sampling points per layer, with a total of 2 layers. The starting position of the sampling points is in the (0, 0, −1) direction (In order to ensure that the sampling points of both the A reference and the B reference are in the same position, in the program, the X-axis is determined through the two holes (90˚ and 270˚) shown in Figure 5. After the part rotates 90˚, these two holes are used to determine the Y-axis). Table 6 shows the measurement values for the other three clamping angles.

Table 6. Measurement values of Datum A flatness, Datum B diameter, and perpendicularity under three clamping angles.

Comparison Dimension	A Evenly Distributed 8 Points, B Single Layer 8 Points, 2 Layers					
	90˚		180˚		270˚	
A Flatness (mm) ▱ 0.02	0.0075	0.0075	0.0100	0.0099	0.0084	0.0084
	0.0076	0.0076	0.0100	0.0100	0.0084	0.0084
A Avg Flatness (mm)	0.0076		0.0100		0.0084	
Range of A Flatness (mm)	0.0001		0.0001		0	
B Diameter ($\phi 58.5_{0}^{+0.05} mm$)	58.5243	58.5242	58.5232	58.5234	58.5224	58.5225
	58.5242	58.5241	58.5235	58.5235	58.5225	58.5224
B Avg Diameter (mm)	58.5242		58.5234		58.5225	
Range of B Diameter (mm)	0.0002		0.0003		0.0001	
B Perpendicularity (mm) ⊥ Ø0Ⓜ A	0.0093	0.0094	0.0013	0.0012	0.0017	0.0016
	0.0093	0.0098	0.0011	0.0007	0.0017	0.0020
B Avg Perpendicularity (mm)	0.0095		0.0011		0.0018	
B Range of B Perpendicularity (mm)	0.0005		0.0006		0.0004	

From the data in Table 6, it can be seen that when the clamping angle remains consistent, the maximum range of Datum A flatness is only 0.0001 mm, the maximum range of Datum B diameter is only 0.0003 mm, and the maximum range of Datum B perpendicularity is only 0.0006 mm, all of which are far less than the equipment's repeatability. Table 7 shows the mean data of Datum A flatness, Datum B diameter, and perpendicularity under the four clamping angles.

Table 7. Mean data of Datum A flatness, Datum B diameter, and perpendicularity under four clamping angles.

Comparison Dimension	A Evenly Distributed 8 Points, B Single Layer 8 Points, 2 Layers			
	0˚	90˚	180˚	270˚
A Avg Flatness (mm) ▱ 0.02	0.0096	0.0076	0.0100	0.0084
B Avg Diameter ($\phi 58.5_{0}^{+0.05} mm$)	58.5232	58.5242	58.5234	58.5225
B Avg Perpendicularity (mm) ⊥ Ø0Ⓜ A	0.0038	0.0095	0.0011	0.0018

From the data in Table 7, it can be seen that after the clamping angle changes, the minimum flatness of Datum A is 0.0076 mm, and the maximum is 0.0100 mm, with a difference of 0.0024 mm, which is slightly greater than the repeatability requirement of the three-coordinate measuring machine; the minimum diameter size of Datum B is 58.5225 mm, and the maximum is 58.5242 mm, with a difference of 0.0017 mm, which is slightly greater than the repeatability requirement of the three-coordinate measuring machine; the minimum perpendicularity of Datum B is 0.0011 mm, and the maximum is 0.0095 mm, with a difference of 0.0084 mm, which is far greater than the repeatability requirement of the three-coordinate measuring machine. The above data shows that the clamping angle has a significant impact on the measurement values.

4.1.5. Standard Part Measurement

After part inspection, the stability of the equipment was verified again using a ring gauge. The reference part was a standard ring gauge, and the reference feature was the parallelism of the upper and lower planes of the ring gauge. With the number and location of sampling points unchanged and only the clamping angle changed, the inspection results showed that the maximum parallelism of the ring gauge was 0.0435 mm, and the minimum was 0.0231 mm, with a difference of 0.0204 mm. Theoretically, the repeatability error for the parallelism of the two planes of the ring gauge should be less than the equipment's repeatability error of 1.5 μm.

4.2. Data Analysis

This experiment was conducted by a dedicated three-coordinate measuring machine inspector, using the same measurement program throughout the inspection process. The environmental conditions met the requirements of the three-coordinate measuring machine, and the same Mo alloy workpiece was used during the detection process. Therefore, the experimental data in this paper excludes possible errors caused by external influencing factors. The reasons for the errors in the data of this paper are analyzed as follows:

1) The measurement values of the A reference plane and the C reference plane's flatness increase as the number of sampling points increases. Theoretically, the more sampling points there are, the better it can reflect the actual state of the part. When the number of sampling points reaches a certain level, the flatness measurement results tend to stabilize. The data in this paper shows that the flatness of both references is increasing and has not yet reached a stable state. Therefore, it is recommended to increase the number of sampling points and continue to verify the relationship between the flatness detection results and the number of sampling points and the sampling point positions.

2) Before and after changes in the sampling point positions and quantities of Datum B and Datum D, the deviations in the diameter detection results of both datums are less than 1 μm. Therefore, this experiment concludes that the three-coordinate measuring machine has the smallest error in detecting cylinder diameters.

3) The Datum B perpendicularity detection process is divided into three rounds. When the number and position of Datum A sampling points change while those

of Datum B remain unchanged, the Datum B perpendicularity measurement value includes the flatness error of Datum A due to the deviation in Datum A flatness. Therefore, the verification results of this round are not convincing. When the number and position of Datum A sampling points remain unchanged while those of Datum B change, the Datum B perpendicularity detection results are also stable because the Datum B diameter detection values are stable. When the Datum A and Datum B states remain unchanged but the clamping angle changes, the difference between the maximum and minimum mean values of Datum B perpendicularity is as high as 0.0084 mm. Combining the measurement values from the above three rounds, it can be seen that the clamping angle has a significant impact on the perpendicularity detection results of the cylinder.

4) When verifying the parallelism of Datum C, due to the influence of the part clamping method, the number and position of sampling points can only be adjusted within half a circular surface. During the detection process, the states of Datum A and Datum B remain unchanged. As the number of Datum C sampling points increases, not only does the flatness of Datum C increase, but the parallelism also gradually increases. Theoretically, when the flatness of a plane increases while the inclination remains unchanged, the parallelism of that plane increases accordingly. The data in **Table 4** is consistent with this phenomenon.

5) Due to the influence of the clamping method, the verification of Datum D position accuracy only adjusts the number and position of sampling points within a semi-cylindrical surface. During the detection process, the states of Datum A and Datum B remain unchanged. The measurement values show that as the number of Datum D sampling points increases, the Datum D position accuracy measurement value shows an increasing trend, but the change is less than 1 μm. The Datum D position accuracy is determined jointly by Datum A, B, and D. Since the states of Datum A and B have not changed, and the change in Datum D diameter is less than 1 μm, the change in Datum D position accuracy is also very small.

5. Conclusions

Through the above analysis, this paper draws the following conclusions:

1) When the surface processing condition of the part is good, the dimensional detection results are not affected by the

2) Even if the surface of the part is in a good processing state, when the number of sampling points and the position of the sampling points change, the measurement values of flatness, parallelism, and position accuracy still have certain deviations. Among them, the detection result of perpendicularity is most affected by the clamping angle.

6. Suggestions and Recommendations

This experiment was affected by the clamping angle, allowing sampling points for Datum C and Datum D only within a half-circle range. It is recommended to design a dedicated fixture for subsequent tests, enabling sampling point detection for Datum C and Datum D on a 0˚ - 360˚ circumference to further assess the impact of the coordinate measuring machine on the measurement results of orientation and location tolerances. The results of this experiment show that the coordinate measuring machine has the greatest impact on orientation tolerances. However, this experiment only verified perpendicularity among orientation tolerances. It is recommended to further verify parallelism and angularity in the future to further verify the stability of the three-coordinate measuring machine's measurement values for orientation tolerances.

Conflicts of Interest

The authors declare no conflicts of interest regarding the publication of this paper.

References

[1] Li, F.Q., Chen, P., Xie, J.Q., *et al.* (2025) Accurate Measurement Method for Geometric Features of Large Radius Small Arcs. *Measurement & Testing Technology*, **45**, 40-47.

[2] Han, J.H., Wang, W., Gong, L.K., *et al.* (2023) Path Planning for Non-Contact Rotating Body Measurement System. *Journal of Changchun University of Science and Technology* (*Natural Science Edition*), **46**, 17-25.

[3] Gong, L.J., Li, X., Zeng, A.M., *et al.* (2025) Three-Coordinate Automatic Detection Technology for Complex Casing Parts. *Metrology & Testing Technology*, **51**, 125-127, 131.

[4] Li, L.B. (2024) Application Research on Error Analysis of Parts Detection Based on Three-Coordinate Measuring Machine. *Internal Combustion Engine & Parts*, No. 19, 71-73.

[5] Zhang, T. (2024) Research on Methods and Application of Detecting Shaft Parts Based on Three-Coordinate Measuring Machine. *Internal Combustion Engine & Parts*, No. 17, 48-50.

[6] Shao, Z.Z. (2023) Reasons for Inconsistent Measurement Results among Three-Coordinate Measuring Machines. *Equipment Management & Maintenance*, No. 2, 66-67.

[7] Zhang, T. (2023) Method and Application of Establishing Coordinate System with Three-Coordinate Measuring Machine. *Journal of Hunan Industry Polytechnic*, **23**, 24-27.

[8] Ye, N.J., Huang, Y.H., Zheng, W.F., *et al.* (202) Research on Accuracy Comparison of Three-Coordinate Measuring Machines. *Metrology & Testing Technology*, **51**, 12-16, 22.

[9] Li, G.L. (2024) Research on Error Compensation of Three-Coordinate Measuring Machine in Precision Machining. *Die & Mould Manufacture*, **24**, 50-52.

[10] Zhang, X.Q., Miao, Y., Jin, Z.H., *et al.* (2025) Application of Three-Coordinate Measuring Machine in Shaft Part Inspection. *Innovation and Application of Science and Technology*, **15**, 184-187.

[11] Tian, F. (2024) Discussion on Reliability of CMM Inspection Results. *Internal Combustion Engine & Parts*, No. 15, 103-105.